# Incorporation of Nonlinearity and Dispersion into Time-Dependent Optical Propagation Models

James E. Toney
Penn State University Electro-Optics Center
222 Northpointe Blvd, Freeport, PA 16229, jtoney@eoc.psu.edu

**Abstract:** The RF/photonics module in Comsol Multiphysics provides complete flexibility in specifying the dielectric function or refractive index as a function of electric field. It is therefore a relatively simple matter to incorporate second-order (second harmonic generation) or third-order (four-wave mixing) nonlinear effects in a qualitative way. However, to move towards practical device modeling, it is essential to include phase mismatch effects, which depend crucially on dispersion. In this paper we show how to incorporate an auxiliary differential equation into a time-dependent EM wave propagation mode to model four-wave mixing in the presence of dispersion. Special cases of this model are used to realize both Lorentz and Drude dispersion models.

**Keywords:** nonlinear optics, dispersion, four-wave mixing, auxiliary differential equation

## 1. Introduction

Second- or third-order nonlinearity can be incorporated into RF/optical propagation models by specifying the polarization as an arbitrary function of the electric field in the subdomain settings. The most general form of the constitutive relation (in the scalar approximation) is:

$$P(E)=P_s+\varepsilon_0(\chi_1 E+\chi_2 E^2+\chi_3 E^3+\ldots) \qquad (1)$$

where $P_s$ is the spontaneous polarization (non-zero for materials with a permanent dipole moment), $\varepsilon_0$ is the permittivity of free space, and $\chi_1$, $\chi_2$, and $\chi_3$ are the first, second and third-order susceptibilities of the material, which are related to the refractive index, second harmonic generation and electro-optic coefficient, and four-wave mixing phenomena respectively. In general, for a two- or three-dimensional model with arbitrary polarization, these quantities are tensors. In this paper we deal with a single field component, so that all quantities can be treated as scalars.

For a centro-symmetric material, $\chi_2=0$, and the constitutive relation can be written as:

$$D=\varepsilon_0\varepsilon_r E+dE^3 \qquad (2)$$

where $\varepsilon_r = n^2 = 1+\chi_1$ is the relative permittivity, n being the refractive index, and $d=\varepsilon_0\chi_3$ is proportional to the nonlinear refractive index, usually written as $n_2$. Expressed this way, the model constitutes a Kerr model for third-order nonlinearity.

The Kerr model does not incorporate dispersion, which is crucial to studying phase matching in devices. To include dispersion along with nonlinearity, one can use a Duffing model, which relates the polarization and electric field via a partial differential equation as[1]

$$\frac{\partial^2 P}{\partial t^2}+2\delta\frac{\partial P}{\partial t}+\omega_0^2(1+\alpha P^2(t))P(t)=\varepsilon_0\chi_1\omega_p^2 E(t) \qquad (3)$$

Here $\omega_0$ is the resonant absorption frequency, $\omega_p$ is the plasma frequency, $\delta$ is a damping factor, and $\alpha$ defines the degree of nonlinearity. (For non-centro-symmetric materials a linear term in P can be included to capture $\chi_2$ effects.) The special case of $\alpha=0$ is the Lorentz model for dispersion in dielectric materials, and the special case of $\alpha=\omega_0=0$ is the Drude model for dispersion in conductive media.[2] This equation can be included as an auxiliary differential equation in a Comsol Multiphysics model via a PDE mode. The dependent variable, P, is then inserted into the constitutive relation of the EM propagation mode to couple the two portions of the model, which are solved simultaneously.

## 2. Model Construction

The second-harmonic generation model from the *Comsol Multiphysics RF Module Model Library* was used as a starting point for a proof-of-concept model. This model uses the 2D, in-plane wave, TE-wave application mode in cylindrical coordinates (z,r,$\phi$). Note this is not a

true axi-symmetric mode, which would constrain the tangential field components to be zero on the symmetry boundary. The tangential component of the vector potential, $A_\phi$, is treated as the dependent variable, and the corresponding electric field is calculated as $E_\phi=-\partial A_\phi/\partial t$.

A PDE mode was added to this model, with the polarization, P, as the dependent variable and coefficients defined according to equation (3). The symbol P was then inserted into the sub-domain properties in the EM mode to link the two parts of the model.

### 2.1 Geometry, Meshing and Boundary Conditions

The geometry consists of a single, rectangular sub-domain. The mesh was defined using a sinusoidal mapping along the input boundary to produce a denser mesh where the field is strongest, exactly as in the second harmonic generation library model.

The top boundary, representing the z-axis (r=0), is taken as a "perfect magnetic conductor" ($H_t=0$) for the EM mode. The bottom boundary is taken as a perfect electric conductor ($E_t=0$). The left (input) boundary uses a scattering boundary condition, with the input field defined as having a Gaussian shape both in space and time. The right (output) boundary uses a scattering boundary condition with zero input field. Note that a scattering boundary is perfectly transparent only for a plane wave, which does not apply in this model. The Gaussian wave front used here does experience significant reflection.

For the PDE mode, it is less clear which boundary conditions are appropriate. For initial studies, we chose the following simple conditions, which produced reasonable results. On the lower boundary, a Dirichlet boundary condition, P=0, was used. On the input boundary, a Neumann boundary condition was used to define P at its linear value:

$$P=\varepsilon_0\omega_p^2\chi_1 E_\phi \qquad (4)$$

On the upper (symmetry) and output boundaries, a null boundary condition was used; that is, a Neumann boundary condition was chosen, with all coefficients equal to zero.

### 2.2 Sub-Domain Properties

In the EM mode, the constitutive relation was chosen to be of the form $D=\varepsilon_0 E+P$, with P being determined by the PDE mode. In the PDE mode, the coefficients were as defined in equation (3), with values for $\omega_0$, $\omega_p$, $\chi_1$ and $\delta$ chosen according to the specific case being studied, as described in Section 3 below.

### 2.3 Solving and Post-processing

Since the frequency spectrum of the output wave is the quantity of interest, a transient solution with fine time steps ($10^{-16}$ s) was computed and Fourier transformed using Comsol Script. The solution as a function of time was recorded for several monitor points along the z-axis.

## 3. Results

To verify that the model produces results that are consistent with known phenomenology, we ran several cases:

1. Nonlinear, no dispersion (equation (2))
2. Linear, Lorentz dispersion ($\alpha=0$; $\omega_0=\omega_p$)
3. Linear, Drude dispersion ($\alpha=\omega_0=0$)
4. Four-wave mixing with dispersion ($\alpha>0$; $\omega_0=\omega_p$)

In each case the behavior of the model was in line with the known physics.

### 3.1 Kerr Model

As a baseline model for four-wave mixing without dispersion, the Comsol second harmonic generation model was modified slightly:

1. the $E_\phi^2$ term in the constitutive relation was replace by $E_\phi^3$ and
2. a second frequency component was added to the input wave

The PDE mode was not included in this case. Because a short propagation distance was used to keep the computation tractable, it was necessary

to use either an unrealistically high value for the nonlinear refractive index or an extremely high field amplitude to see significant frequency conversion. With $d \sim 10^{-32}$-$10^{-31}$ Cm/V$^3$, which corresponds to a realistic value of $n_2 \sim 10^{-19}$-$10^{-18}$ m$^2$/W, a field amplitude on the order of $10^9$ V/m was necessary.

Figure 1 shows input and output spectra; a degenerate four-wave mixing peak is clearly visible at $f_3=2f_1-f_2$ in the output.[3]

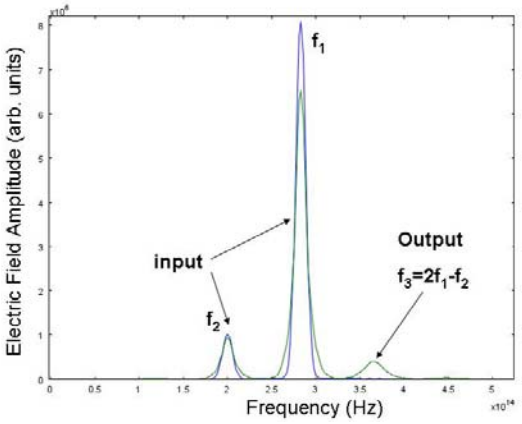


**Figure 1**. Input and output spectra showing four-wave mixing using Kerr model.

### 3.2 Lorentz Dispersion

To realize a Lorentz model for dispersion, it is only necessary to set $\alpha=0$ and $\omega_0=\omega_p$ in equation (3). There are two ways to verify this model: launch a broad-band pulse and observe its spreading, or set $\omega_0$ equal to the frequency of the input wave and observe the strong absorption at this resonant frequency. For the first method, the input wave must be near the resonant frequency where dispersion is greatest, so that significant spreading can be seen within a limited propagation distance. A representative result for $\omega_0=1.2\ \omega_{in}$ is shown in Figure 2; from comparison of the time waveforms at the input (blue), middle (green) and output (red) monitor points, broadening of the pulse during propagation is evident.

Figure 3 shows the transmission spectrum for the case in which the resonant frequency is equal to the frequency of the pump wave. For this example the damping parameter, $\delta$, was set equal to $\omega_0/100$, producing a rather sharp absorption peak. Clearly there is strong attenuation at $f_1=\omega_0/2\pi$, while the probe wave at $f_2$ is largely unaffected, as expected.

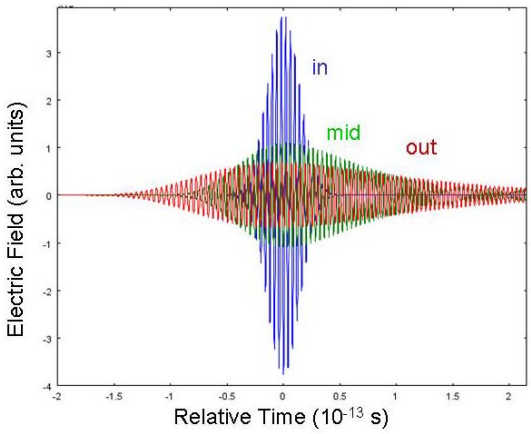


**Figure 2**. Pulse spreading due to Lorentz dispersion with $\omega_0=1.2\ \omega_{in}$

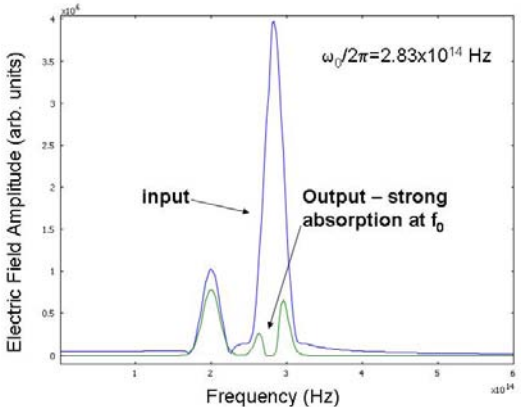


**Figure 3**. Input and output spectra using Lorentz model.

### 3.3 Drude Dispersion

To implement Drude dispersion, we set $\omega_0=0$ and $\chi_1=1$ in equation (3). The expected behavior in this case is that waves at a frequency substantially greater than the plasma frequency, $f_p=\omega_p/2\pi$, will propagate freely, while lower-frequency waves will be reflected or absorbed.

A simple way to verify the proper function of the Drude model is to propagate the same two frequency components as in the previous examples, with several different values of the

plasma frequency. Figure 4 shows the transmission spectrum for four cases: $f_p<<f_2<f_1$, $f_p<f_2<f_1$, $f_2<f_p<f_1$ and $f_p>f_1>f_2$. Clearly as $f_p$ increases, the attenuation increases, first for the lower frequency component then for the higher one; when $f_p>f_1$ there is negligible transmission.

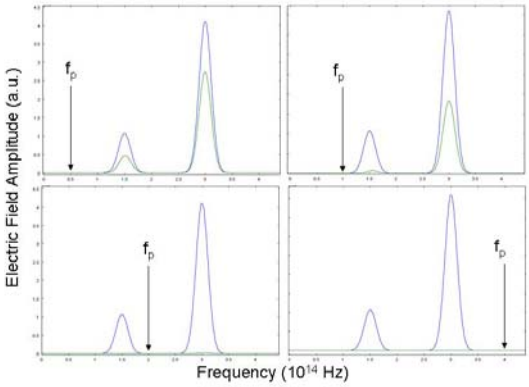


**Figure 4**. Input (blue) and output (green) spectra using Drude model with several values of the plasma frequency.

### 3.4 Duffing Model

For the general case of dispersion with nonlinearity, we choose $\omega_p=\omega_0$ to be in the near-UV region ($2\pi c/\omega_0$ = 0.3-0.4 μm) and $\chi_1=1$ ($n=\sqrt{2}$), corresponding to a typical glass.

To choose a suitable value for α, it can be related to the more familiar nonlinear refractive index of the Kerr model ($n_2$) as[1]

$$\alpha = -\frac{n_0 n_2}{\varepsilon_0^2 \chi_1^3 \eta_0} \qquad (6)$$

where $\eta_0 = (\mu_0/\varepsilon_0)^{1/2}$ is the impedance of free space.

Figure 5 shows the output spectrum for this case on a logarithmic scale, revealing that in addition to the four-wave mixing peaks at $2f_1$-$f_2$ and $2f_2$-$f_1$, there are third-harmonic-generation peaks and higher-order processes.

The affect of dispersion on phase matching can be seen by plotting the power in the four-wave mixing peak at $2f_2$-$f_1$ vs. propagation distance. Figure 6 shows the FWM power relative to the probe ($f_2$) power vs. propagation distance for three values of $\omega_0$. As the resonant frequency decreases, thereby increasing the dispersion in the frequency range around $f_1$ and $f_2$, the transfer length and maximum transferred power decrease. This result shows that dispersion is exerting a critical influence on the phase mismatch.

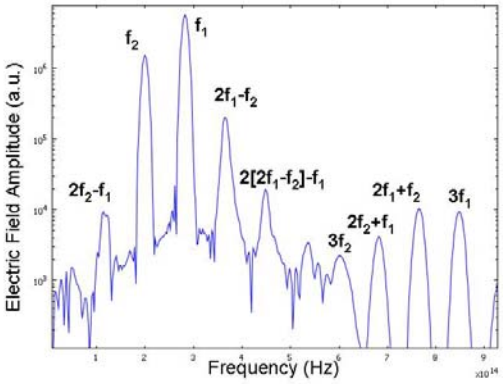


**Figure 5**. Output spectrum for Duffing model with input frequencies at $f_1$ and $f_2$.

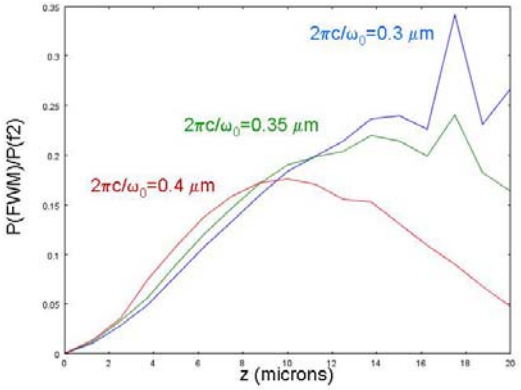


**Figure 6**. Power in FWM peak relative to probe wave vs. propagation distance for several values of the resonant frequency.

## 4. Extensions of the Model

The model described here can be extended in several ways to handle other cases. First, $\chi_2$ effects such as second-harmonic generation can be incorporated by including an additional term in equation (3) so that the restoring force becomes $\omega_0^2[1+\beta P(t)+\alpha P(t)^2]P(t)$. The value of β in terms of the usual nonlinear optical coefficient, $d_{11}$, is:

$$\beta=-d_{11}/(\varepsilon_0\chi_1)^2 \qquad (7)$$

To incorporate both Drude (electron) and Lorentz (lattice) contributions to the dispersion, with the latter potentially having multiple resonances, a separate PDE mode can be added for each contribution, $P_i$, to the polarization density. In the EM mode, the total polarization density would then be specified as $P=P_D+\Sigma P_{L,i}$, where $P_D$ is the Drude contribution and $P_{L,i}$ is the ith Lorentz term.

Extension of the model to three dimensions can be accomplished by specifying the polarization as a vector (p1 p2 p3) upon creation of the PDE mode. All coefficients can then be entered as tensors. However relating the coefficients of equation (3) to the dielectric and nonlinear optical tensors for anisotropic materials requires further analysis that is beyond the scope of this paper.

## 5. Conclusions

We have demonstrated a unified model for dispersion and nonlinearity that can be incorporated into any Comsol Multiphysics electromagnetic propagation model via a PDE mode. By appropriate choice of parameters, the model has been verified to produce the correct phenomenology for Lorentz and Drude dispersion, as well as four-wave mixing in the presence of dispersion.

## 6. References


1. V. Janyani, A. Vukovic, J. D. Paul, P. Sewell, T. M. Benson, "The Development of TLM Models for Nonlinear Optics," *Microwave Review* **10,** 35 (2004)
2. M. Bordovsky, P. Catrysse, S. Dods, M. Freitas, J. Klein, L. Kotacka, V. Tzolov, I. Uzunov, J. Zhang, "Waveguide Design, Modelling, and Optimization – from Photonic Nano-devices to Integrated Photonic Circuits," *Proc. SPIE* 5355, 65 (2004)
3. O. Aso, M. Tadakuma, S. Namiki, "Four-Wave Mixing in Optical Fibers and Its Applications," *Furukawa Review* **19**, 68 (2000)